886 *KSME International Journal, Vol. 13, No. 12, pp. 886~904, 1999*

A Target-Approachable Force-Guided Control with Adaptive Accommodation for Complex Assembly

Sungchul Kang*, Munsang Kim*, Chong-won Lee* and Kyo-Il Lee**

(Received Jannary 11, 1999)

In this paper, a target approachable force-guided control with adaptive accommodation for complex assembly is presented. Complex assembly (CA) is defined as a task which deals with complex shaped parts including concavity, or whose environment is so complex that unexpected contacts occur frequently during insertion. CA tasks are encountered frequently in the field of manufacturing automation and various robot applications. To make CA successful, both the bounded wrench condition and the target approachability condition should be satisfied simultaneously during insertion. The bounded wrench condition can be satisfied by properly designing accommodation parameters, which depends on the tolerable stiffness for an assembly task, not to exceed the prescribed contact wrench. On the other hand, the target approachability condition can be satisfied by determining an admissible twist minimizing the deviation between the current and target twist. By applying convex optimization techniques, an optimum target approaching twist can be determined at each instantaneous contact state as a global minimum solution. Incorporated with an admissible perturbation method, a new CA algorithm using only the sensed resultant wrench and the target twist is developed without motion planning or contact analysis (which requires the geometry of the part and the environment). To verify the feasibility of the new assembly algorithm, a wench sensor model based on a minimum distance algorithm has been developed and used to estimate contact wrenches in graphic assembly simulation. Finally, a VME bus-based real-time control system is built for experiments on various CA tasks. The T-insertion task as a planar CA, and the double-peg assembly task as a spatial CA, were successfully executed by implementing the new force-guided control with adaptive accommodation.

Key Words : Robotic Assembly, Complex Assembly, Twist, Wrench, Target Approachability, Bounded Wrench, Adaptive Accommodation Control, Compliance, Real-time Control

1. Introduction

Among manufacturing processes, assembly process is one of the most labor-intensive sectors in which the share of the cost of the assembly can amount from 25 to 75 percent of the total production costs(Rampersad, 1994). Therefore, assembly process is very important in the manufacturing automation field, and many researchers have been studying the automation of the assembly process using robots. However, aside from simple peg-in-hole-like insertion processes such as electronic component assembly, which allow larger tolerance than the robot's positioning accuracy, many assembly processes are not automated. The main reason is that, in many assembly processes, the robot's positioning errors or the misalignment between the assembly parts can make the assembly operation fail in some ceses even causing damage to the assembly parts. To solve these problems, *active* compliant motion control approaches have been intensively studied and implemented together with *passive* approaches

* Korea Institute of Science and Technology
P. O. BOX 131, Cheongryang, Seoul, Korea
Tel: +82-2-958-5589
Fax: +82-2-958-5629
Email: kasch@kistmail. kist. re. kr
** School of Mechanical and Aerospace Engineering, Seoul National Univ., Seoul 151-742, KOREA

which use a remote centered compliance (RCC) device attached to the robot end-effector (Whitney, 1982). In addition to simple assembly (or fixturing) processes in manufacturing, various robot applications, e. g., construction, component repair in space or in hazardous environments, and robotic surgery, require a technique for the insertion of a complicated object into a positionally uncertain environment. In these applications, the shape of the part inserted is not simple, and the environment geometry may also not be exactly known.

In this work, a complex assembly (CA) is defined as a task which deals with complex, possibly concave shaped parts, and whose environment is so complex that unexpected contacts occur frequently during insertion. Unlike conventional peg-in-hole tasks, CA has the feature that the dimension of the nominal insertion path can usually be more than one, and the contact states occurring during insertion for CA are various and complicated. Therefore, due to the computational complexity of generating a multi-dimensional motion plan, conventional compliant motion planning approaches based on various existing compliant control schemes have limitations when applied to CA. Moreover, they cannot represent nonlinear compliance effects resulting from multi-contact cases occurring more frequently and severely in the CA process.

Recently, several results related to CA have been presented by extending existing active compliance approaches. Shimmels and Peshkin (Peshkin, 1990, Shimmels and Peshkin, 1992, Shimmels and Peshkin, 1994) proposed an admittance control law for force-guided assembly applicable to a typical fixture assembly task with or without friction. By using the least square approximation method, an admittance controller which guarantees both the bounded force condition and the error reducible condition is designed. Also, they derived a force-assemblable condition based on the *linear* compliance mapping. The method requires a contact analysis for every possible contact state occurring in fixture assembly. Due to the limitations of linear compliance mappings (Asada, 1993), although all possible contact states can be generated from the geometry of the part and environment (Xiao and Zhang, 1997), in practure the method is difficult to apply to CA tasks which deal with complex parts with concavities and whose contact states are complicated and change severely. In other words, the linear compliance (or accommodation) mapping, which maps the contact wrench (force/torque) into the position (or velocity), is not usually appropriate for representing multi-contact cases occurring in the CA process.

McCarragher (McCarragher and Asada, 1995a, McCarragher and Asada, 1995b) presented a discrete event controller by imitating the human decision making mechanism for assembly tasks, and successfully experimented on two complex peg-in-hole tasks, e. g., dual peg and two-tied peg insertion tasks. Also, the control system includes a qualitative matching process (McCarragher and Asada, 1993) to monitor the current contact state during assembly. However, similar to the work of Shimmels and Peshkin's, since it requires the geometry of all possible contact states to build a petri net as a discrete event system model, the more complex the geometry of the parts becomes, the more complicated and time-consuming the task of building the petri net becomes. Moreover, since it needs numerical procedures to compute the optimal discrete event trajectory and optimal continuous insertion path during assembly, it does not seem to be computationally effective or appropriate for high speed assembly tasks.

As another active compliant control approach, Lee and Asada (Lee and Asada, 1997) presented perturbation/correlation method using a vibratory end-effector. The correlation between the lateral perturbation generated from the piezo-actuator and the longitudinal reaction force sensed from the F/T sensor gives information on the insertion direction minimizing the reaction force. However, since it was motivated from the task of inserting a long pipe into a stack of thin sheet metals, whose inner surface of the hole is irregular and rugged, the dimension of the nominal insertion path is limited to one. Therefore, in the case of a CA task requiring both translational and rotational mo-

tion with multi-dimensions, it would be difficult to extract the valid information from the multi-dimensional cross-coupled correlation between the perturbation motions and the sensed force/torque.

Kang et al. (Kang, Hwang, Kim et al., 1997, Kang, Hwang, Kim, et. al, 1998a) presented a Cartesian stiffness controller which uses the rotational degree of freedom effectively during insertion by dynamically updating the location of the compliance frame to the current contact point. To compensate for the error between the planned and the actual position of the contact point, a contact localization method using the F/T sensor information and the geometry of the inserted part is adopted. The proposed stiffness controller was successfully implemented to a real-time controller and tested on a T-insertion task involving tight tolerances. However, the controller can only handle single-contact cases to simplify the localization procedure, since it is difficult to uniquely localize the instant center of rotation (or compliance center) in multi-contact states. Moreover, the computation time of the localization procedure depends on the complexity of the shape of the inserted part (Kang, Hwang, Kim, et. al, 1998b)

On the other hand, several compliant motion planning methods have been presented. As a higher-level approach than those described above, compliant motion planners produce compliant motions allowing contact assuming that various compliant motion controllers, such as a damping controller, hybrid position/force controller and impedance controller, are implemented at the servo level. Lozano-Perez, et al. (Lozano-Perez, Mason and Taylor, 1984) introduces the concept of uncertainty cones to develop a planning methodology called backprojection. In this paradigm, motion is planned backward from the goal region toward the start point. For a given goal region, the uncertainty cone is used to compute a backprojection region such that if the robot starts to move in the commanded direction from this region, it is guaranteed to reach the goal region. This computation is recursively done until the start point is included in one of the backprojection regions. The notions of goal recognizability and termination conditions are also important in compliant motion planning since the robot joint encoder readings alone cannot tell whether the goal is reached and when to stop motion commands. A number of results have followed (Latombe, Lazanas and Shekar, 1991), and the current status can be summarized as 1) the complexity of motion planning under uncertainty is exponential in the number of backprojection steps(Canny, 1989), 2) the backprojection regions are not unique and depend on the termination condition(Erdmann, 1986) and 3) implementation is very difficult beyond for dimensions (Brost and Christiansen, 1994). Most of these methods assume that the positional accuracy degrades as the travel distance increases.

As described above, most existing compliant control and planning approaches usually are not easily applicable to CA due to their dependency on the part geometry or on the dimension of the motion, since they require contact kinematic analysis procedures for every possible contact, or planning procedures to produce a path for compliant motion. To solve these complexity problems inherent in CA, a geometry independent force-guided control with target approachability to a desired mating position is needed. Target approachability, which is a key idea in this work, causes the inserted part to move closer to the prescribed target pose in the admissible motion space constrained by the contact wrench. Using the target approachability condition as the man criterion for CA, a differential twist minimizing the deviation between the current and the target twist constrained by repelling or reciprocal conditions (Ohwovoriole and Roth, 1981) can be determined. To make CA successful while satisfying the target approachability condition, the bounded wrench condition (Peshkin, 1990) should also be satisfied at every contact state during insertion not to exert a larger wrench than the tolerable one. The bounded wrench condition can be satisfied by properly designing the accommodation parameters go as not to exceed the prescribed contact wrench. To solve the optimum twist at a contact state, an optimization problem

statement is formulated. To build the optimization problem, the square of the norm of the twist deviation between the current and the target twist is defined as an objective function, and the repelling/reciprocal conditions as an inequality constraint function. Using the Kuhn-Tucker conditions from convex optimization theory(Arora, 1989), an optimum target approaching twist can be determined as a global minimum solution at each instantaneous contact state. Therefore, using the convex optimization technique incorporated with an admissible perturbation method, a new force-guided control with adaptive accommodation algorithm using only a sensed resultant wrench and an updated target twist can be developed without motion planning or a contact kinematic analysis procedure requiring the geometry of the part and the environment. Through simulations and experiments on a variety of CA tasks including T-insertion and double-peg-assembly, its feasibility and applicability are verified.

2. Approach to Complex Assembly

2.1 Definition of complex assembly

A conceptual example of CA is illustrated in Fig. 1. Fig. 1 shows an assembly which handles a complex shaped part in a complex environment. Different from simple peg-in-hole tasks, CA has the feature that the dimension of the nominal insertion path is usually more than one, and the contact states during insertion are various and complicated.

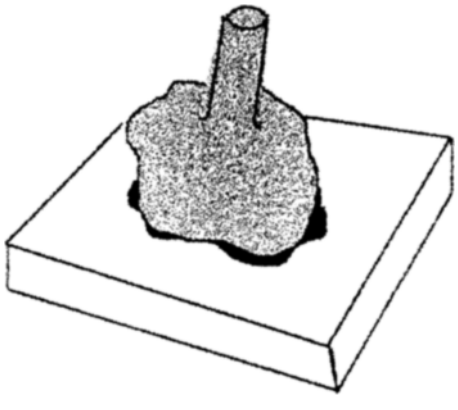

Fig. 1 Complex Assemly

In this study, the complex assembly process is assumed to handle complex-shaped objects. The complex-shaped object (CSO) is defined as Definition 1.

Definition 1 *A complex-shaped object is defined as an object whose geometry is composed of polyhedra including concavities.* Using Definition 1, a complex assembly (CA) task is defined as follows.

Definition 2 *A complex assembly is an insertion task whose part and(or) environment include(s) CSO(s).*

The CA operation has either a one-dimesional or multi-dimensional path as a nominal insertion path depending on the geometry of the part (or the environment) and the initial pose (position/orientation) of the inserted part. The double-peg and the two-tied peg insertion problems(McCarragher and Asada, 1995) can be categorized as a complex assembly with a one-dimensional nominal path, since their geometry include concavities. Complex assembly also has many more possible contact states including multi-contact ones than the simple peg-in-hole problem due to the complex geometry.

2.2 Complex assembly algorithm

As a first step to formulaing the CA algorithm in this work, we assume that there is neither a nominal motion plan nor prescribed contact states analyzed from the geometry of the part and environment. This assumption corresponds to the situation where a blindfolded human inserts a part into a hole without any geometric information of the part and the hole. In this situation contact states occur unexpectedly due to the geometric complexity or the misalignment between the part and the environment. When the situation is transferred to a robot assembly system, the information usually available to the robot are 1) the end point position/orientation, 2) the sensed *resultant* contact wrench(force/torque) and 3) target position/orientation with uncertainty.

When there is no planned nominal path for insertion, the error reducible property (Peshkin, 1990) is no longer meaningful. Rather, target

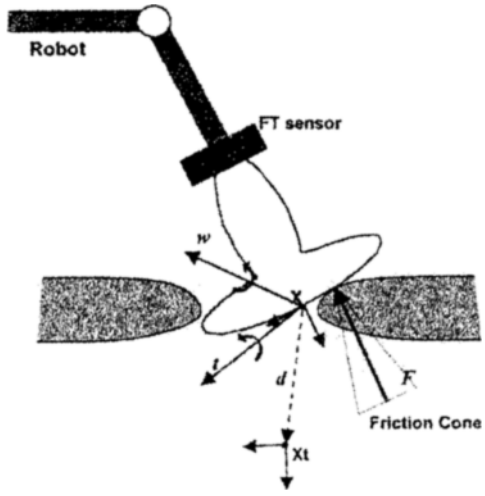

Fig. 2 Target approaching twist in contact

approachability (Kang, Kim, Lee, et. al, 1998c) is valid, which is to make the inserted part move closer to a known target point in the admissible motion space constrained by the constraints due to contacts.

At a contact state during a typical CA task shown in Fig. 2, a differential twist (translational and angular velocities) which minimizes the deviation between a target twist and an admissible twist satisfying the reciprocal and the repelling conditions (Ohwovoriole and Roth, 1981) is defined as a *target approaching twist*. According to screw theory(Ball, 1900), the reciprocal and the repelling constraints representing the admissible motion space in contact are described by a resultant contact wrench w and a differential twist t in inequality form as follows :

$$g(t) = -w^T t \leq 0. \tag{1}$$

where $w = (\tau_x, \tau_y, \tau_z, f_x, f_y, f_z)^T$ and $t = (\omega_x, \omega_y, \omega_z, \nu_x, \nu_y, \nu_z)^T$.

Physically, inequality (1) means that an object in contact can move either in the reciprocal motion space$(-w^T t = 0)$ or in the repelling motion space $(-w^T t < 0)$. The reciprocal motion space corresponds to the pace in which the virtual work computed from the exerting wrench and the displacement is equal to 0, while the reciprocal motion space corresponds to the pace in which the virtual work computed from the wrench and the displacement is greater than 0.

Note that both the wrench and twist are described in the (Tool Center Point) TCP frame, which is described as X in Fig. 2. The resultant wrench measured in a FT sensor can be transformed to that in the TCP frame by using the static equilibrium relation of forces and moments.

The objective function $f(t)$ is defined as a half of the square of the normed deviation between the *target twist* d determined from the current(X) to the target position/orientation(Xt) and the unknown differential twist t. The target twist d is also a vector in the TCP frame, to maintain consistency with the current and the target pose vectors described in the TCP frame.

A pose (position/orientation) vector X is described as follows :

$$X = (P^T, O^T)^T, \tag{2}$$

where $P = (x, y, z)^T$ and $O = (\alpha, \beta, \gamma)^T$.

The magnitude of the target twist is given by desired translational V_d and Ω_d angular velocities commanded by a user. Thus the target twist d is represented as

$$\begin{aligned} d &= (\omega_{dx}, \omega_{dy}, \omega_{dz}, \nu_{dx}, \nu_{dy}, \nu_{dz})^T \\ &= (\omega_d^T, \nu_d^T)^T \end{aligned} \tag{3}$$

where $\omega_d = (O_t - O)/\|O_t - O\| \cdot \Omega_d$ and $\nu_d = (P_t - P)/\|P_t - P\| \cdot V_d$.

Therefore, the objective function is described as

$$f(t) = \frac{1}{2}\|d - t\|^2. \tag{4}$$

Both the quadratic objective function $f(t)$ and constraint function $g(t)$ are convex functions since the Hessian matrix of each function is positive-semi-definite(Arora, 1989). Therefore, this is a convex optimization problem which guarantees a global minimum at an instantaneous quasi-static contact state. Finally, the CA problem can be formulated as a simple quadratic convex optimization to find a target approachable twist t^* as follows :

Find a twist t^* *which minimizes* $f(t) = \frac{1}{2}\|d - t\|^2$ *subject to* $g(t) = -w^T t \leq 0$.

To make the objective function represent both the deviation of the translational twist and the

difference of the rotational twist, a metric on the space of twist deviations needs to be defined. It is not obvious how the metric should be defined to balance the difference between translation and rotation. To balance the magnitude of the translational twist and the rotational twist with the same unit (mm) in this study, the rotational twist vector is scaled by multiplying a weighting radius of rotation. The weighting radius of rotation is defined as a maximum radius of rotation of the inserted object.

By applying the Kuhn-Tucker conditions for the optimization problem with inequality constraints, the Lagrange function L is described as

$$L=f(t)+u\cdot g(t). \tag{5}$$

Then there exists a Lagrange multiplier u^* such that the Lagrangian is stationary with respect to each twist component t_i, *i.e.* v_x, v_y, v_z, ω_x, ω_y, ω_z and u as follows.

$$\frac{\partial L}{\partial t_i}\equiv\frac{\partial f}{\partial t_i}+u^*\frac{\partial g}{\partial t_i}=0, \tag{6}$$

$$g(t^*)\le 0. \tag{7}$$

$$u^*\cdot g(t^*)=0 \text{ and} \tag{8}$$

$$u^*\ge 0. \tag{9}$$

2.3 Adaptive accommodation law

It is important to note that condition (8) can be divided into two cases, which are $u^*=0$ and $g(t^*)=0$. When $u^*=0$, the inequality constraint is inactive. Thus the optimum target approaching twist is simply the same as d. In this case, the contact wrench does not constrain the part to be inserted to the target pose. This case corresponds to the situation illustrated in Fig. 3. Figure 3(a) shows the physical situation during a planar CA task. The optimum twist lies in the repelling motion space. Figure 3(b) shows the optimum within the differential twist vector space in a 3-dimensional planar CA problem. The optimum twist t^* is determined from (6) as follows:

$$t^*=d. \tag{10}$$

In the other case that $g(t^*)=0$, in which the inequality constraint is active at the contact state as shown in Fig. 4(a), the optimum twist is in the reciprocal motion space as shown in Fig. 4(b). In this case, the optimum twist t^* can be solved simultaneously from (6)-(9) as follows :

$$t^*=d+u^*\cdot w \tag{11}$$

where $u^*=-w^Td/\|w\|^2\ge 0$.

It is important to note that the Lagrange multiplier u^* maps the sensed resultant wrench into the target approaching twist in cooperated with the dynamically updated target twist d. Thus u^* has accommodation characteristics similar to the conventional damping control law. However,

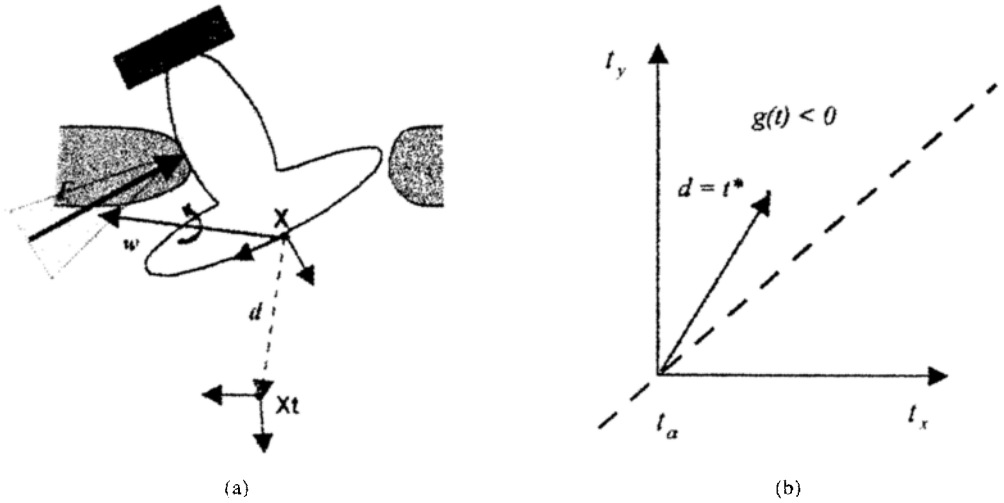

(a) (b)

(a) Corresponding contact state in planar CA task
(b) Optimum twist t^* in the repelling motion space(projected to 2-dim. plane)

Fig. 3 Optimum by repelling motion

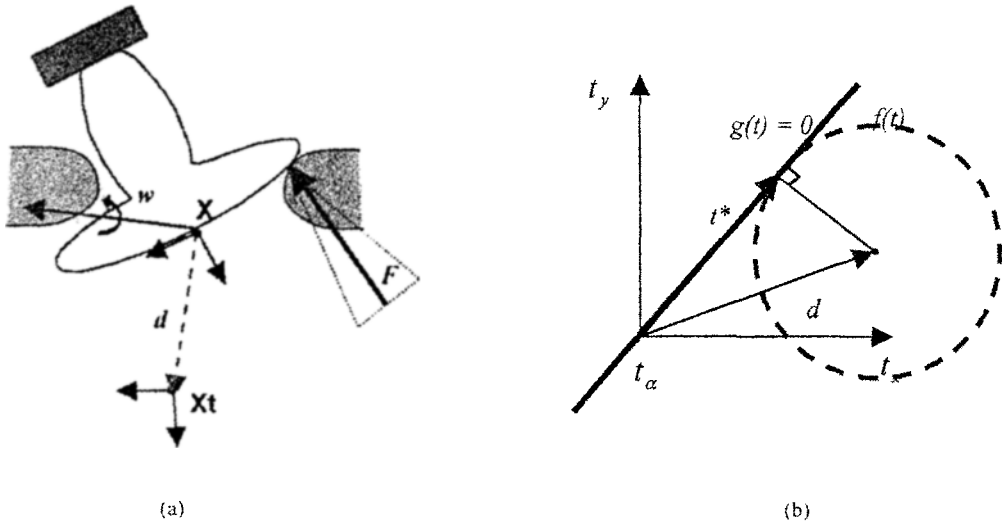

(a) (b)

(a) Corresponding contact state in CA task
(b) Optimum twist t^* in the reciprocal motion space(projected to 2-dim. plane)

Fig. 4 Optimum by repelling motion

in contrast to the conventional accommodation matrices, which are usually linear mappings and determined in the least-square sense, the Lagrange multiplier u^*, which is a scalar, determines an optimum target approaching twist dynamically using the sensed current resultant wrench and the current target twist d. Therefore, the optimum twist Eq. (11) has adaptive accommodation, characteristics which dynamically changes the mapping depending on the current contact wrench and the target twist. Thus the new control law described in (11) together with (10) is called an "*adaptive accommodation law*" in this study.

The condition $u^* \geq 0$, which guarantees the existence of the optimum solution, is a necessary condition for determining whether a target approaching twist exists. If $u^* < 0$, there is no optimum solution and thus a target approaching twist does not exist. Therefore, u^* is an important index indicating that the target approachability condition is satisfied at a contact state. Thus in this study it is called an "*accommodation index*."

The optimum target approaching twist t^* lies in the reciprocal motion space and thus does not have an explicit compliance property which ensures the bounded forces at the contact point(s). Moreover in some multi-contact cases whose admissible motion space cannot be constructed

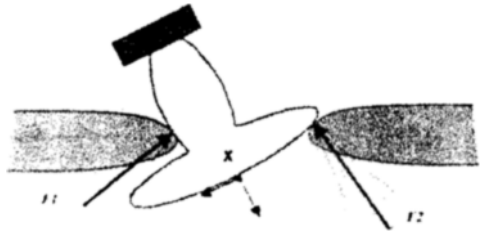

Fig. 5 Multi-contact example in CA process

correctly only using the resultant wrench, the optimum twist determined in the motion space cannot guarantee target approachability. To solve this problem, a perturbation twist method which determines a twist making the resultant contact wrench not exceed the prescribed bound of the contact wrench is required. The perturbation twist method is synthesized as follows.

2.4 Perturbation twist in the virtual admissible motion space

In a multi-contact case occurring in a CA process as shown in Fig. 5, the admissible motion space (AMS) constrained by the reciprocal and the repelling constraints is determined as the intersection of the spaces of the admissible motion resulting from each contact wrench (Hirai and Asada, 1993).

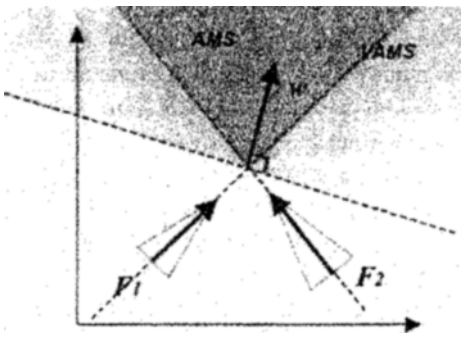

Fig. 6 Difference between AMS and VAMS

However, the AMS can only be determined from the contact analysis depending on the geometry of the part and environment at each contact. Thus the motion space built by the resultant wrench sensed by the F/T sensor strictly differs from the admissible motion space. The motion space from the resultant wrench, however, usually includes the AMS since the space built by the resultant wrench is an expanded space of the admissible motion space. We call this space a *virtual admissible motion space* (VAMS). For a simple planar multi-contact example shown in Fig. 6, the AMS is a subset of VAMS. For the sake of simplicity in the illustration, Fig. 6 shows only the planar translational motion space formed by the contact forces F_1 and F_2.

In the adaptive accommodation control law, the optimum twist determined from the resultant wrench may not exist in the AMS but in the VAMS. Therefore, if it does not exist in the AMS, the optimum twist obtained from the Kuhn-Tucker conditions cannot guarantee target approachability. Rather, it can even make the part exert a large wrench to the environment, making a dangerous contact situation. To prevent this problem, the bounded wrench condition should be added to the accommodation controller. That is, when the magnitude of the sensed resultant wrench exceeds the wrench limit in case of an ill-conditioned contact state, a twist perturbation in the direction of the wrench within the VAMS is generated to find a direction making the sensed wrench bounded. As a result of repetitive perturbations in VAMS, the part can be moved to a different contact state (or a non-contact state) which may be possible to proceed with insertion. Especially in the case of a jamming (or wedging) situation due to a multi-contact with large friction, the rotational perturbation in the same direction as that of the sensed torque vector is effective since it tends to change the contact state to a different one or to a non-contact state. This concept can be formulated by using the conventional damping control law. The translational perturbation twist vector δ_V is modeled as

$$\delta_V = diag(C_V,\ C_V,\ C_V) \cdot f \tag{12}$$

In Eq. (12), $diag(C_V,\ C_V,\ C_V)$ is a diagonal matrix (3×3) whose diagonal components are all C_V's. Based on the damping control method, C_V is a constant accommodation parameter offering a translational compliance in contact. The magnitude of the C_V can be determined from the inverse of the tolerable translational stiffness K_V at the robot end-point and the sampling time T_S for the controller as follows :

$$C_V = \frac{1}{K_V T_S}. \tag{13}$$

The tolerable stiffness K_V can be estimated from the desired robot end point stiffness and the measurable range of the FT sensor.

On the other hand, the rotational perturbation twist vector δ_ω is also modeled by the sensed resultant torque vector $\tau = (\tau_x,\ \tau_y,\ \tau_z)$ as

$$\delta_\omega = diag(C_\omega,\ C_\omega,\ C_\omega) \cdot \tau \tag{14}$$

Similar to Eq. 5 13), $diag(C_\omega,\ C_\omega,\ C_\omega)$ is a diagonal matrix (3×3) whose diagonal components are all C_ω's. C_ω is also a constant accommodation parameter for rotational compliance. The magnitude of the C_ω can be designed in the same way as follows :

$$C_\omega = \frac{1}{K_\omega T_S}. \tag{15}$$

Finally, a six-dimensional perturbation twist vector δ is described in VAMS as follows :

$$\delta = (\delta_V^T,\ \delta_\omega^T)^T. \tag{16}$$

Consequently, the perturbation twist δ is computed from the sensed resultant wrench to proceed with insertion while maintaining the tolerable magnitude of the resultant contact wren-

ch, when the value of the accommodation index is less than 0 or the sensed resultant wrench is larger than the prescribed wrench bound during CA.

3. Controller Design

Based on the accommodation(or damping) control approach which maps the contact wrench into the twist to produce an accommodation effect (or an admittance), the adaptive accommodation controller is designed.

During insertion, if the norm of the sensed resultant wrench is below the prescribed contact wrench value, i. e., contact is not detected, the target twist d is directly commended to the position controller as a desired position/orientation command. The conventional PID (Proportional -Integral-Derivative) controller is used as a basic position controller. On the other hand, in the case that contact(s) is detected, the d is input to the TAF module to determine the target approaching twist t with respect to the TCP frame. Once t is determined in the TAF module, it is used to update the desired pose vector X_d, which is commanded to the position controller. The desired Cartesian pose command X_d is updated from d if any contact is not detected from the force/torque sensor, while X_d is updated from t if a contact is detected.

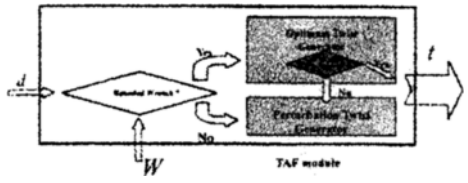

Fig. 7 Target approchable force-guided(TAF) module

When a contact is detected during insertion, the TAF module is activated and computes a target approaching twist as either optimum twist generator or perturbation twist generator. The block diagram of the TAF module is as shown in Fig. 7.

In summary, the proposed TAF control system has three control modes : the non-contact mode, the optimum twist mode, and perturbation twist mode. In the non-contact twist mode, the controller performs like a free-space position controller to approach the commanded target pose. When contact is detected, the optimum twist mode or perturbation twist mode is activated. If the accommodation index is zero or positive and the bounded resultant wrench condition is satisfied, the optimum twist mode is activated in the TAF module. On the other hand, if either the accommodation index or the bounded resultant wrench condition is not satisfied, the perturbation twist mode is activated to determine the perturbation twist vector.

Unlike the accommodation matrix (Peshkin, 1990) based on linear mappings, our adaptive accommodation controller has nonlinear characteristics as represented in (10) and (11). The algorithm for solving an optimum twist which is analytically derived in (10) and (11), and the perturbation generation module can be simply implemented as an external feedback loop. The accommodation parameters C_V and C_ω used to generate perturbations should be designed carefully by taking into account the tolerable stiffness of the part and environment, and the bandwidth of the robot. The overall block diagram of the proposed TAF control system for CA is shown in Fig. 8.

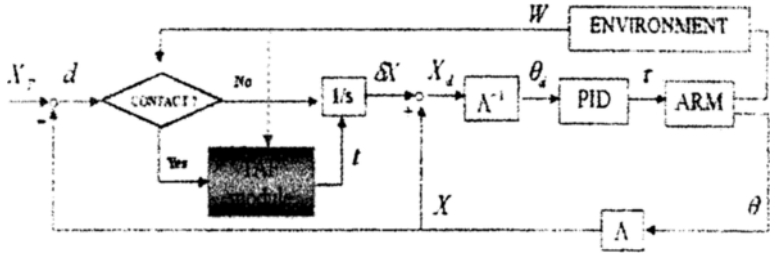

Fig. 8 Block diagram of target approachable control system for CA

4. Simulation

The designed TAF controller needs a simulation stage to verify its feasibility and to estimate the accommodation parameters before it is implemented to a robot control hardware for experiment.

As an important module for the simulation of compliant motion, a force/torque sensor model (Schilling, 1990) is needed to compute the contact wrench from the penetration depth between the assembly parts. To compute the penetration depth in contact state in a graphic environment, several algorithms for computing the penetration depth have been presented as an extended work of the computation of the minimum distance between polyhedral objects (Gilbert, Johnson and Keerthi, 1988). However, the penetration depth algorithm is not used in this work since it is thought to be on-going work (Gilbert and Ong, 1994) and is not a main focus of this study. Rather, an approximated penetration depth is computed by effectively applying a minimum distance algorithm.

To compute the approximated penetration depth to determine the contact wrench in contact between polyhedral objects, the minimum distance function provided by IGRIP (Interactive Graphic Robot Instruction Program) (Deneb Robotics Inc., 1994) is used. IGRIP is a commercial robot simulation package which has a variety of robot simulation functions including CAD modeling, kinematics, dynamics, control, etc.

As the object O_1 moves as shown in Fig. 9, when it penetrates object O_2 due to discrete motion in the graphic environment, it can be interpreted as contact occuring in the physical world. Although the penetration depth does not exist between rigid bodies in contact, it can be used to virtually compute the contact forces in the simulation world. The penetration depth between objects O_1 and O_2, can be computed approximately by extending the minimum distance algorithm. In other words, when contact occurs between O_1 and O_2, the moving object O_1 virtually retrocedes by a smaller step size in the negative direction of the previous minimum distance vector untill the minimum distance becomes non-zero. The previous minimum distance vector is the one which was saved immediately before the contact. Note that the step size of the virtually retroceding motion should be sufficiently smaller than that of the normal motion to ensure that the retroceding motion feasibly approximate the perturbation depth.

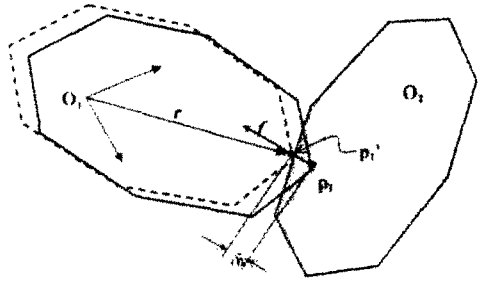

Fig. 9 Contact wrench determined from penetration depth

The contact force vector with respect to frame O_1 can be determined from the penetration depth and the retroceding vector. The retroceding vector is the negative of the previous minimum distance vector s_p, which has been determined with respect to frame O_1 before the contact. Thus the contact force equation can be described as follows :

$$f = -K \cdot \delta x \cdot s_p \tag{17}$$

where K is the object stiffness.

Also the friction force model can be added by using the friction cone concept formulated in quasi-static contact. Assuming that the static Coulomb friction coefficient μ is constant, the friction forces orthogonal to the contact force f can be randomly determined within the friction cone.

The moment vector m with repect to frame O_1 can also be determined from f as

$$m = r \times f \tag{18}$$

where r is the position vector of p_1' with respect to the frame O_1. The p_1' is the retorceded point until the minmum distance becomes non-zero. Finally, the contact wrench w is expressed as

$$w = (f^T,\ m^T)^T. \tag{19}$$

In the multi-contact case, the resultant contact wrench can be determined by summing the wrenches from each contact. Since the object geometry used in this wrench sensing model is assumed to be a convex polyhedron, the concave object should be modeled as an union of convex polyhedra. Therefore the resultant wrench W in the multi-contact case can be described as

$$W=\sum_{i=1}^{n} w_i \tag{20}$$

where n is the number of contacts and w_i is the contact wrench of i-th contact.

Consequently, the wrench sensing model is developed by the minimum distance algorithm without computing the penetration depth directly. The force vector is not an exact one but an approximated one since it is determined by retorceding in the direction of the previous minimum distance vector. However, the approximated force vector is sufficiently feasible to compute the contact wrench as long as the approaching motion is smooth.

As a prior step for the CA experiment, both T-insertion and double-peg assembly simulations are performed in IGRIP as shown in Fig. 10.

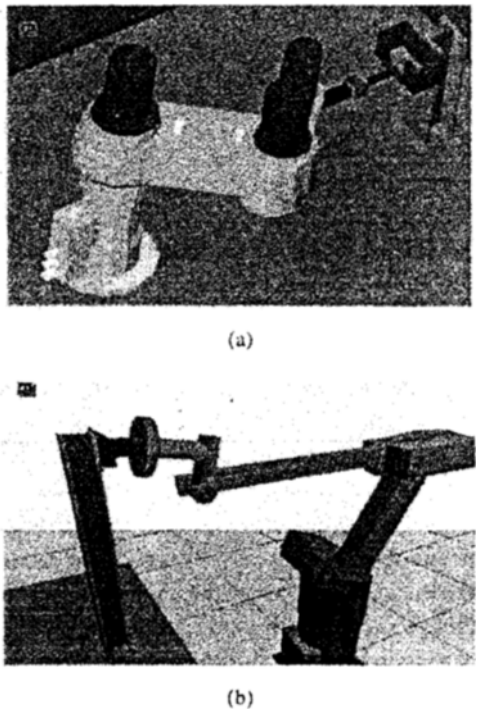

Fig. 10 CA simulation: T-insertion and Double-peg assembly

5. Experiment

5.1 Robot control system for CA

A variety of CA tasks which have been verified in the CA simulation stage are experimented by using the VME based real-time robot control system called HUROCOS (Humanoid Robot Control System). HUROCOS, which runs in a real-time OS (VxWorks) is a general-purpose robot control system aimed at building a

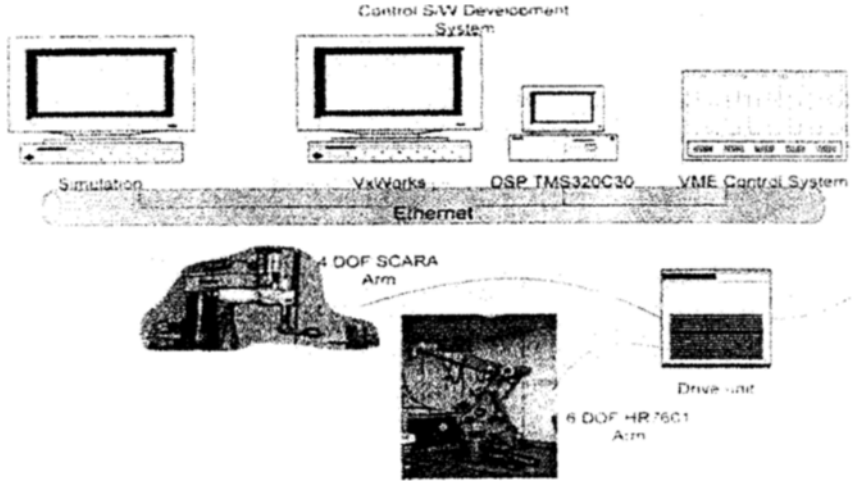

Fig. 11 VME-based real time robot control system

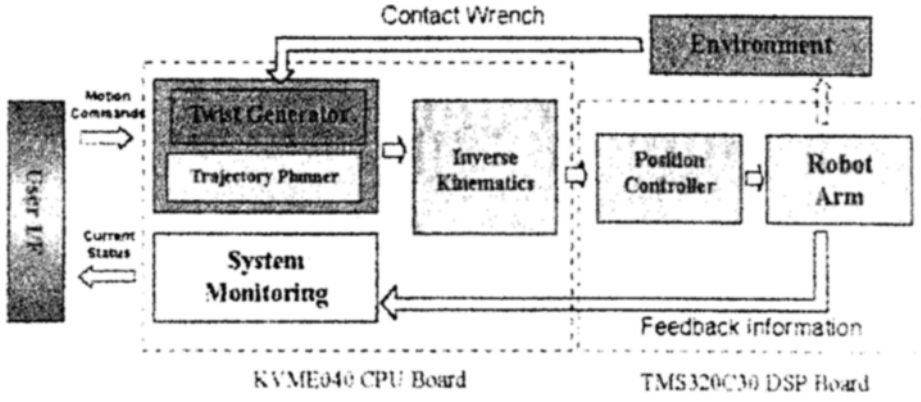

Fig. 12 Information flow in the robot control software

humanoid robot called CENTAUR (Lee, Kim, Hong, et. al, 1998) developed at Korea Institute of Science and Technology (KIST). The overall hardware structure of HUROCOS is shown in Fig. 11. To share the computational loads, the HUROCOS hardware is composed of two types of control platform ; a KVME040 CPU board performs the computation for trajectory generation, inverse kinematics, F/T sensor interface, user interface and system monitoring. This KVME040 board plays a supervising role since it can read/write data on the other slave boards via a VME bus by accessing dual-port RAM. On the other hand, the multi-functional motion control board with TMS320C30 DSP, which was developed at KIST, handles the computation for PID servo control in joint space, digital I/O interface and joint encoder feedback. It can control 4 robot joints simultaneously.

To access the sensed forces/torque data from the KVME040 board, the JR3 VME-bus receiver board is used. The force/torque data which are filtered and AD-converted in the F/T sensor body, are written to the dual-port RAM in the receiver board via RS485 serial communication. The force/torque data transferred to the dual-port RAM can be accessed easily by the KVME040 via VME-bus.

Two commercial industrial robot manipulators controlled by our HUROCOS are used for planar and spatial CA tasks. The original control system of industrial robots is not an open-architecture system, and thus various control algorithms such as the CA algorithm cannot implemented easily. Therefore, we interfaced HUROCOS with industrial robot manipulators. Each of the manipulators can be controlled in the HUROCOS environment by only changing its kinematic structure.

The software structure and the information flow in the robot control software is illustrated in Fig. 12. The set of HUROCOS control commands include three types of commands : motion commands, inquiry commands, and set commands. HUROCOS can execute a robot by issuing several motion commands, can access feedback information given by the FT sensor and joint encoders, and can set position control gains and the power status. Among the control commands, the complex assembly task is executed by issuing the motion command "*Complex Assembly*" with the necessary parameters on the HUROCOS operation terminal. Several important control commands are listed in Table. 1.

In summary, we have built a real-time robot control system for various CA experiments. By developing our own software/hardware for the control system, both the flexibility and the open architecture are realized. With this control system, several complex assembly tasks have been attempted. We begin the experimental result sections with a T-insertion task, which is a planar assembly task.

5.2 T-insertion

As a typical example of planar CA, which uses rotational motion effectively to insert a T-shaped

Table 1 HUROCOS control commands

Commany Type	Command Name	Input Paramenters
Motion	*InitArm*	*(int ArmID);*
	MoveArmToHome	*(int ArmID, int HomeID, float Time);*
	MoveArmAbsJoint	*(int ArmID, AJoint Jtarget, float Time);*
	MoveArmRelJoint	*(int ArmID, AJoint Jtarget, float Time);*
	MoveArmAbsWorld	*(int ArmID, Frame Ftarget, float Time);*
	MoveArmRelWorld	*(int ArmID, Frame Ftarget, float Time);*
	ComplexAssembly	*(int ArmID, Frame Ftarget, float Des Tw, float MaxTime);*
Inquiry	*ReadArmFTsensor*	*(int ArmID, FTsensor *FTval);*
	ReadStatus	*(int ArmID, AJoint *Jval, Frame *Fval);*
	ReadArmControlGain	*(int ArmID, int Gnum);*
Set	*SetArmControlGain*	*(int ArmID, int Gnum);*
	PowerEnable	*(int ArmID)*
	PowerDisable	*(int ArmID);*
	SetArmHomeFrame	*(int ArmID, int HomeID);*

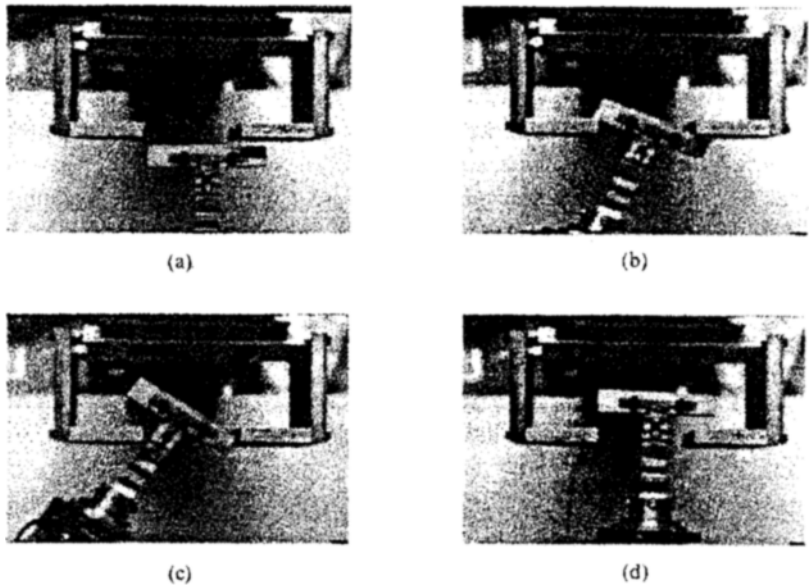

Fig. 13 T-insertion experiment result

part into the target pose, a T-insertion task is implemented and experimented by the robot control system described above.

The robot used in the T insertion is a Goldstar GHR350-Ⅱ SCARA robot which is similar to an Adept robot. To make the robot move in X, Y and α directions in the TCP frame during T insertion, it has been reconstructed to 3-DOF by freezing the third prismatic joint. The high-performance hardware architecture has achieved a

trajectory update rate of 500 Hz since the inverse kinematics is so simple that its analytical solution can be obtained easily.

Both the T-shaped part and C-shaped box have the same dimensions as those used in the simulation stage. The result of the experiment is illustrated in sequential photographs in Fig. 13.

The specifications required to execute the insertion task is listed Table. 2. The trajectory (twist)

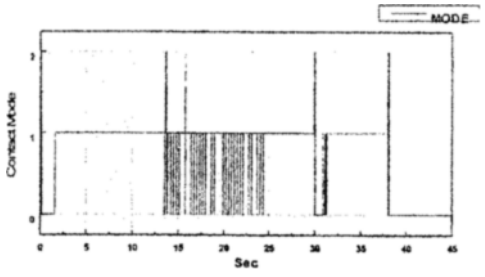

Fig. 14 Contact modes during insertion

update rate is assigned by considering the computation time for the twist generation and the inverse kinematics of the robot. In the case of the planar robot, the inverse kinematics is so simple that the trajectory update rate can be increased up to 2 msec. The servo rate in the PID controller is also set by considering the steady state response of the robot dynamics.

The result of the T-insertion experiment is shown sequentially from Fig. 13(a) to Fig. 13(d). Figure 13(a) shows an initial position of T. The initial position is set to ensure an approaching direction to the target position where the insertion is completed. There is no limitation to the initial position unless it causes a sticking state which the target approachability is not satisfied in terms of the accommodation index. From the contact mode plot shown in Fig. 14, almost contact modes are the optimum twist mode (1) due to the

Table 2 Task specification data for T-insertion

Task specification		Value
Intial pose in base frame (x, y, $roll$)		(620 mm, −0.5 mm, 0 rad)
Target pose in TCP frame (x, y, $roll$)		(50 mm, 0.5 mm, 0 rad)
Trajectory update rate(Ts)		2 msec
Servo rate(ts)		1 msec
Tolerable Stiffness at TCP(Kd)	Translational	150 N/mm
	Rotational	200.000 N*mm/rad
Desired Twsit(t_d)	Translational	50 mm/sec
	Rotational	1.2 rad/sec

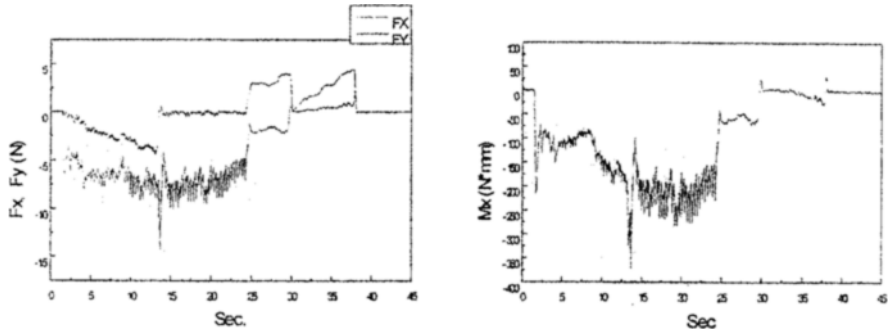

Fig. 15 Sensed resultant wrench

Table 3 Task specification data for double-peg assembly

Task specification		Value
Intial pose in base frame (*x, y, yaw, pitch, roll*)		−44 mm, 790 mm, 1453 mm, 85 deg, 0 deg, 180 deg)
Target pose in base frame (*x, y, yaw, pitch, roll*)		(−37 mm, 890 mm, 1454 mm, 85 deg, −1.5 deg, 180 deg)
Trajectory update rate(Ts)		6 msec
Servo rate(ts)		1 msec
Tolerable Stiffness at TCP(Kd)	Translational	200 N/mm
	Rotational	10,000 N*mm/rad
Desired Twsit(t_d)	Translational	25 mm/sec
	Rotational	15 rad/sec

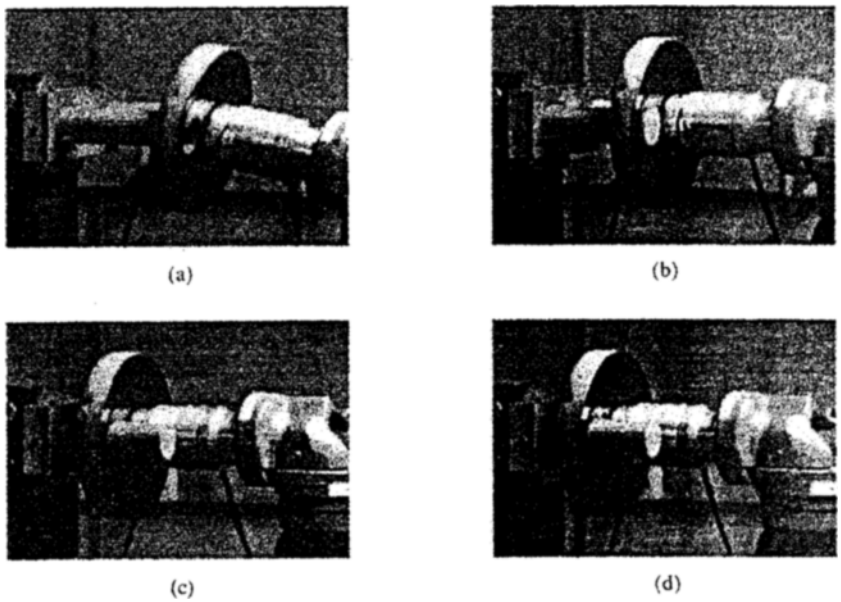

Fig. 16 Experiment result: Double-peg assembly

adaptive accommodation property. In the perturbation twist mode (2), which usually corresponds to a multi-contact case, the perturbed motion helps to disengage the jamming condition by changing the current contact state to another state. Figure 15 shows the resultant forces and torque measured by F/T sensor during insertion. From the tolerable stiffness specified in Table 2, the measured forces and torques satisfy the bounded wrench property which offers compliance in contact.

5.3 Double-peg assembly

As a second example of complex assembly to verity the adaptive accommodation controller, a double-peg assembly task has been experimented. This experiment can be thought of as a simple example for the wheel assembly operation in a car manufacturing line which inserts a wheel with 4 holes into a hub with 4 pegs. However, the radial tolerance of this assembly is set small enough to ensure that the proposed controller can be applied to various precision assembly tasks involv-

ing complex geometry.

Even though this task has parts with complex geometry, the nominal insertion path is one-dimensional motion. Therefore, the insertion operation can be successfully executed by the conventional compliant motion control approaches such as damping control, stiffness (or impedance) control, and hybrid position/force control as long as the initial misalignment is so small that it can be covered by the compliance property provided by the controllers. However, when the amount of misalignment is so large, the conventional compliant controller cannot alleviate the effect of the misalignment and canse insertion failure because they do not possess target approachability using the adaptive accommodation property.

This double-peg assembly experiment focuses on robustness against the initial misalignment for the successful insertion. This experiment is for showing that assembly is possible as long as the resultant wrench can represent the admissible motion approaching the target position even though the parts geometry is complex. In the double-peg assembly example, if the initial pose is set so that the two pegs are partially inserted into the holes, and thus the resultant wrench can easily find an admissible motion to the target position, the assembly operation is successful regardless of the geometric complexity of the parts.

The task specification for the double-peg assembly with initial misalignment is listed in Table 3. As shown in Fig. 16(a) and specified in Table 3, a rotational misalignment in pitch direction in the base frame, which amounts to 15 degrees, is given to the initial condition. As a result of generating the optimum twist and the perturbation twist to approach the target position, the assembly was executed successfully in spite of the misalignments. Figure 16 shows the sequential result of the assembly operation.

Figure 17 shows the contact modes experienced during the insertion. Due to the small tolerance (0.1 mm), the free non-contact modes are scarcely shown during the insertion stage after the mating stage overcoming the misalignment is completed. The double hole disk tries to be inserted against the misalignment by interchanging its contact mode among free, optimum, and perturbation modes. This motion can be seen from 0 until 5 sec in Fig. 17. Once the disk is inserted after 5 sec, the inserting motion interchanges between the optimum mode and the perturbation mode. It means that during this time the disk can be inserted by a simple compliant motion just like a single peg-in-hole task. Figure 18 shows the bounded wrench property subject the prescribed tolerable stiffness specified in Table 3.

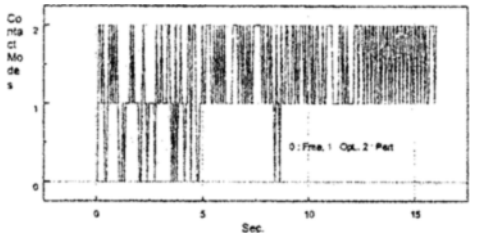

Fig. 17 Contact modes during insertion

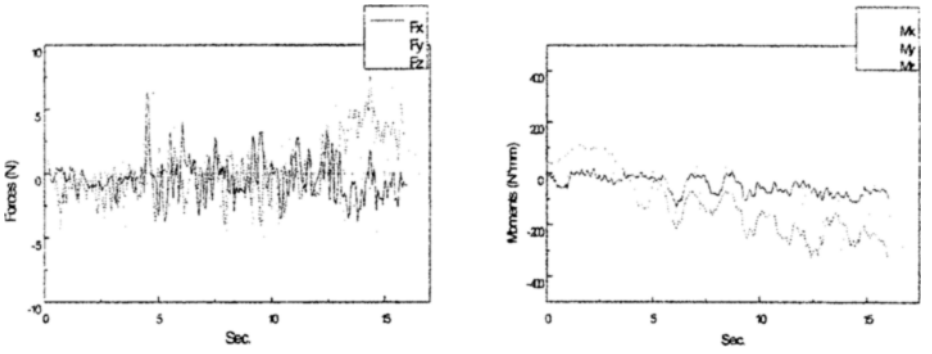

Fig. 18 Sensed resultant wrench

6. Conclusions

In this work, complex assembly(CA) is newly defined as a result of the investigation of various assembly tasks encountered in industry and the other automation fields. By examining the CA operation demonstrated by a blindfolded human, a simple assembly rule called the adaptive accommodation law, which imitates human operation, is exploited and mathematically formulated using twists and wrenches. To attempt automation for CA tasks using a robot with a force/torque sensor, a new geometry-independent adaptive accommodation control is developed by modeling the complex assembly operation as a convex optimization problem, which includes an updated target twist and a current resultant contact wrench. The goal of the optimization is to achieve both target approachability and the bounded wrench property at each contact state during insertion. The contact states are represented as the repelling and the reciprocal constraints derived by screw theory and used as an inequality constraint for the optimization framework. Additionally, the admissible perturbation method which generates a twist in the virtual admissible motion space constructed from the sensed resultant wrench is proposed to make the contact wrench bounded and to disengage the unexpected jamming (or wedging) condition. Since both the optimum twist generator and the perturbation twist generator do not require any geometry information of the parts or the environment, the control algorithm can be easily implemented to various complex assembly tasks.

The adaptive accommodation control law has been verified by graphic simulation prior to being implemented to the control hardware. By computing the virtual contact wrench using the penetration depth approximately determined from the minimum distance, a novel wrench sensor model has been developed in the IGRIP graphic simulation environment.

As well as the peg-in-hole task, a variety of complex assembly tasks such as T-insertion and double peg assembly have been successfully implemented and executed in a VME-based real-time robot control system, which is a general purpose robot controller developed for the humanoid robot project at the Korea Institute of Science and Technology.

In the near future, integrated with a vision system for global motion planning, the adaptive accommodation controller is planned to be applied to practical complex assembly tasks, especially those in car manufacturing lines, which have not been automated yet due to the complexity of the geometry of the part and environment. Furthermore this work is expected to be easily extended to a cooperative assembly task using two arms, which is more human-like and efficient in terms of the measure of time and energy, since the adaptive accommodation control algorithm is independent of the geometry of the assembled parts, the number of the contact states, and the structure of the robot kinematics.

References

Arora, 1989, *Introduction to Optimum Design*, McGraw-Hill, Singapore.

Asada, H., 1993, "Representation and Learning of Nonlinear Compliance Using Neural Nets," *IEEE Trans. Robotics and Automation*, Vol. 9, No. 6, pp. 863~867.

Ball, R. S., 1900, *A Treatise on the Theory of Screws*, Cambridge University Press, Cambridge.

Brost, R. C. and Christiansen, A. D., 1994, *Probabilistic analysis of manipulation tasks: A computational framework*, Technical Report SAND92-2033, Sandia National Laboratories, Albuquerque, NM.

Canny, J. F., 1998, "On computability of the fine motion plan," *Proc. of the IEEE Int. Conf. On Robotics and Automation*, pp. 177~182.

Deneb Robotics Inc., 1994, *IGRIP Graphic Simulation Language (GSL) Reference Manual*.

Erdmann, M., 1986, "Using backprojection for the fine motion planning with uncertainty," *Int. J. Robotics research*, Res. 5 (1), pp. 19~45.

Gilbert, E. G., Johnson, D. W. and Keerthi, S. S., 1988, "A Fasr Procedure for computing the Distance Between Complex Objects in Tree-

Dimensional Space," *IEEE Journal of Robotics and Automation*, Vol. 4, No. 2, pp. 193~203.

Gilbert, E. G. and Ong, C. J., 1994, "New Distance for the Separation and Penetration of Objects," *Proc. IEEE Int. Conf. Robotics and Automation*, pp. 579~586.

Hirai, S. and Asada, H., 1993, "Kinematics and Statics of Manipulation Using the Theory of Polyhedral Convex Cones," *The International Journal of Robotics Research*, Vol. 12, No. 5, pp. 434~447.

Hwang, Y. K., Kang, S., Lee, S., Park, S., Cho, K., Kim H. and C. W. Lee, 1998, "Human Interface, Automatic Planning and Control of a Humanoid Robot," *International Journal of Robotics Research*, Vol. 17, No. 11, pp. 1131~1149.

Kang, S., Hwang, Y. K., Kim, M. Lee, K. and Lee, C., 1997, "A Compliant Motion Control for Insertion of Complex Shaped Objects using Contact," *Proc. IEEE Int. Conf. Robotics and Automation*, pp. 841~846.

Kang, S., Hwang, Yong K., Kim, Mun S. and Lee, Kyo I. 1998, "Assembly of Complex Shaped Objects : A Stiffness Control with Contact Localization," *KSME Journal*, Vol. 12, No. 3, pp. 451~460.

Kang, S., Hwang, Yong K., Kim, Mun S. and Lee, Kyo I. and Lee, C., 1998, "A Compliant Controller Dynamically Updating the Compliance Center by Contact Localization," *Robotica*, Vol. 16, part 5, pp. 543~550.

Kang, S., Kim, M., Lee, C. W. and Lee, K., 1998, "A Target Approachable Force-Guided Control for Complex Assembly," Proc. IEEE Int. Conf. Robotics and Automation, pp. 826~831, Leuven, Belgium.

Latombe, J. C., Lazanas, A. and Shekhar, S., 1991, "Robot motion planning with uncertainty in control and sensing,'" *Artificial Intelligence*, Vol. 52, pp. 1~47.

Lee, S. and Asada, H., 1997, "Assembly Automation using Vibratory End Effector : Modeling and Stability Analysis," *Proc. IEEE Int. Conf. Robotics and Automation*, pp. 1980~1985.

Lee, C. W., Kim, M. S., Hong, Y. S., et. al. 1998, *Development of Humanoid Robot System*, Korea Institute of Science and Technology, Annual Report.

Lozano-Perez, M. T. Mason and R. H Taylor, 1984, "Automatic Synthesis of Fine Motion Strategies for Robotics," *International Journal of Robotics and Research*, Res. 3 (1), pp. 3~24.

Peshkin, M. A., 1990, "Programmed Compliance for Error Corrective Assembly," *IEEE Trans. Robotics and Automation*, Vol. 6, No. 4, pp. 473~482.

McCarragher, B. J. and Asada, H., 1995, "The Discrete Event Control of Robotic Assembly Tasks," *ASME Journal of Dynamic systems, Meas. And Control*, Vol. 117, pp. 384~393.

McCarragher, B. J. and Asada, H., 1995, "The Discrete Event Modeling and Trajectory Planning of Robotic Assembly Tasks," *ASME Journal of Dynamic systems, Measurement and Control*, Vol. 117, pp. 394~400.

McCarragher, B. J. and Asada, H., 1993, "Qualitative Template Matching Using Dynamic Process Models for State Transition Recognition of Robotic Assembly," *ASME Journal of Dynamic Systems, Measurement and Control*, Vol. 115, pp. 261~269.

Ohwovoriole, M. S. and Roth, B., 1981, "An Extension of Screw Theory," *Journal of Mechanical Design*, Vol. 103, October, pp. 725~735.

Rampersad, H. K., 1994, *Integrated and Simultaneous Design for Robotic Assembly*, John Wiley, Chichester.

Schilling, R. J., 1990, *Fundamentals of Robotics : Analysis and Control*, Prentice Hall, New York.

Shimmels, J. M. and Peshkin, M. A., 1992, "Admittance Matrix Design for Force-Guided Assembly," *IEEE Trans. Robotics and Automation*, Vol. 8, No. 2, pp. 213~227.

Shimmels, J. M. and Peshkin, M. A., 1994, "Force Assembly with Friction," *IEEE Trans. Robotics and Automation*, Vol. 10, No. 4, pp. 465~479.

Whitney, D. E., 1982, "Quasi-Static Assembly of Compliantly Supported Rigid Parts," *Journal of Dynamic Systems, Measurement and Con-*

trol, Vol. 104, pp. 65~77.

Xiao, J. and Zhang, L., 1997, "Contact Constraint Analysis and Determination of Geometrically Valid Contact Formations from Possible Contact Primitives," *IEEE Trans. of Robotics and Automation*, Vol. 13, No. 3, pp. 456~466.